Geosystems and Geoenvironment 4 (2025) 100379

Contents lists available at ScienceDirect

Geosystems and Geoenvironment

journal homepage: www.elsevier.com/locate/geogeo

Ozone patterns in Maceió: Insights into seasonal and geographic varibility

Amaury de Souza[a], Celina M. Takemura[b], Deniz Özonur[c], Elias Silva de Medeiros[d], Ivana Pobocikova[e], Janice F. Leivas[b], José Francisco de Oliveira-Júnior[f], Kelvy Rosalvo Alencar Cardoso[f], Marcel Carvalho Abreu[g], Wagner Alessandro Pansera[h], Jose Roberto Zenteno Jimenez[i], Sneha Gautam[j,*]

[a] Federal University of Mato Grosso do Sul, Campo Grande, Brazil
[b] Embrapa Territory, Campinas, SP, Brazil
[c] Gazi University, Ankara, Turkey
[d] Federal University of Grande Dourados, Brazil
[e] Faculty of Mechanical Engineering, University of Zilina, Slovakia
[f] Federal University of Alagoas, Maceió, Brazil
[g] Federal Rural University of Rio de Janeiro, Seropédica, Rio de Janeiro, Brazil
[h] Universidade Tecnológica Federal do Paraná-UTFPR, Toledo, PR, Brazil
[i] Ingenieria Geofisica Instituto Politecnico Nacional Ciudad de Mexico, ESIA Unidad Ticoman, Depto. de Ingenieria Petrolera., Mexico
[j] Karunya Institute of Technology and Science, Coimbatore 641 114, Tamil Nadu, India

ARTICLE INFO

Article history:
Received 7 November 2024
Revised 14 February 2025
Accepted 26 February 2025

Handling Editor: Sanzhong Li

Keywords:
Ozone
Seasonal variability
Anthropogenic factors
Air quality
Brazil

ABSTRACT

This study analyzes the Total Ozone Column (TCO) over six cities in Alagoas, Brazil, aiming to evaluate their spatial and temporal homogeneity and identify seasonal and annual patterns from 2008 to 2016. TCO is a key indicator for monitoring the ozone layer and its implications for public health, given ozone's role in filtering ultraviolet radiation. The analysis utilized satellite-derived TCO data, with variance homogeneity assessed using the Bartlett test at a 95% significance level. Descriptive statistical analyses characterized the temporal distribution of TCO values, and probability density functions (PDFs) identified the best-fitting statistical distribution.

The findings indicate significant homogeneity in annual and seasonal TCO concentrations, with an annual mean of 263.24 ± 9.91 DU. A biannual TCO cycle was observed, with peaks in spring and lows in fall, influenced by Earth's orbit and ozone photochemistry. The data were best represented by a normal distribution, reflecting the role of the Brewer-Dobson Circulation in maintaining ozone uniformity and mitigating disruptions from phenomena like the Antarctic Polar Vortex.

These results emphasize the need for continuous monitoring of ozone variability, as fluctuations in TCO can affect ultraviolet radiation levels and, consequently, public health outcomes such as skin cancer and ocular diseases. The study underscores the importance of integrating TCO data into environmental policies and public health strategies, particularly in regions with high solar radiation exposure. The study's limited statistical sensitivity and geographic coverage highlight the necessity of further research on factors influencing ozone distribution and its broader environmental and health implications.

1. Introduction

Atmospheric ozone is essential for the Earth's radiative balance and for protection against UV-B radiation harmful to living things (Kim and Newchurch, 1998; Kim et al., 2013; Gilford and Solomon, 2017). Changes in ozone concentration affect atmospheric dynamics, influencing cloudiness, cyclone frequency, Hadley cell expansion, and precipitation patterns (Grise et al., 2014, 2013). Ozone variability is driven by ozone-depleting substances (Steinbrecht et al., 2018; Weber et al., 2018) and dynamic factors like ENSO and the Quasi-Biennial Oscillation (QBO; Toihir et al., 2018).

* Corresponding author.
E-mail address: snehagautam@karunya.edu (S. Gautam).

https://doi.org/10.1016/j.geogeo.2025.100379

Interannual variability impacts the Brewer-Dobson Circulation, which moves ozone from the tropics to the poles (Albers et al., 2018; Diallo et al., 2018). Studies indicate that phenomena such as ENSO play a crucial role in modulating ozone concentrations, and it is essential to understand how these dynamics affect the Total Ozone Column (TCO), especially in vulnerable regions such as the Northeast of Brazil (NEB), where sun exposure is intense (Xie et al., 2014; Zhang et al., 2015, 2019). Recent research investigates the variability of TCO at different geographic and temporal scales, examining the influence of natural and anthropogenic factors. Coldewey-Egbers et al. (2022) analyzed the global TCO from 1995 to 2020, highlighting regional variations and the influence of ENSO (El Niño-Southern Oscillation). They noted that while ozone recovery in the upper stratosphere is ongoing, trends in the lower stratosphere are still uncertain. Wang et al. (2024a) found that TCO variability in southwestern Europe (2010–2021) is influenced by natural factors and human activities like industrial emissions and traffic.

Long-term ozone monitoring is vital to evaluate the Montreal Protocol's impact. Although ODS levels have dropped, global ozone recovery trends remain statistically insignificant (Braesicke et al., 2018). Interannual ozone variability, especially at mid- and high-latitudes, may mask these trends, and feedback mechanisms with climate change may introduce additional variations (Coldewey-Egbers et al., 2022; Wang et al., 2024b).

Evolution of the ozone in the troposphere, particularly in the tropics, complicates the determination of the overall trend in TCO, with regional increases observed due to factors such as ENSO (Wang et al., 2023, 2024b). ESA's CCI and EU's C3S generate climate data, enabling better analysis and understanding of ozone dynamics. This study uses TCO data collected between 2008 and 2016 by the OMI sensor aboard the Aura satellite. The goal is to assess TCO trends and distribution in Alagoas, enhancing understanding of regional air quality and atmospheric impacts.

2. Methodology

2.1. Field site and data collection

The study area covers latitudes 09°19′06″ S to 10°07′32″ S and longitudes 35°33′ 40″ W to 37°26′12″ W, with an average altitude of about 100 meters above sea level, as shown in Fig. 1. OMI sensor data from the Aura satellite (Jan 2008-Dec 2016) were used. Table 1 provides geographic coordinates (latitude and longitude), altitude, and statistical summaries of TCO in all municipalities. TCO measurements are performed using solar radiation spectrometry and advanced algorithms, which are essential for interpreting data and formulating effective air pollution control strategies (Levelt et al., 2006a, 2006b; Souza et al., 2021). These methods not only help identify pollution sources, such as O_3 and NO_2, but are also essential for analyzing the spatiotemporal variability of ozone. Algorithms such as the following are used to interpret satellite data: TOMS Total Ozone Algorithm (TOA) – Used by the TOMS (Total Ozone Mapping Spectrometer) sensor, this algorithm estimates TCO from the absorption of ultraviolet radiation at multiple wavelengths. Dobson and Brewer Spectrophotometers Calibration Algorithms – These methods are applied to calibrate ozone sensor data, ensuring greater measurement accuracy. OMI DOAS (Differential Optical Absorption Spectroscopy) – Implemented in the OMI (Ozone Monitoring Instrument) sensor, this algorithm detects TCO through the differential absorption of sunlight reflected by the atmosphere, improving the analysis of the spatial distribution of ozone. Optimal Estimation Method (OEM) – an algorithm based on Bayesian inference widely used in the recovery of vertical ozone profiles, allowing the differentiation between stratospheric and tropospheric layers. Machine learning-based retrievals – modern ap-

Table 1
Geographic coordinates, population, area and statistics of average daily TCO concentrations in municipalities during the period (2008–2016), derived from measurements by the OMI sensor on board the Aura satellite.

City	Latitude (S)	Longitude (W)	Altitude (m)	Population	Area (km^2)	Average (DU)	SD	CV (%)	Min (DU)	Max (DU)	N
3. Arapiraca	09°45′09″	36°39′40″	264	233,047	345.655	263.04	9.88	3.76	236	304	2710
24. Coruripe	10°07′32″	36°10′32″	16	57,294	897.800	263.32	9.87	3.75	236.8	310.6	2717
68. Pão de Açúcar	9°44′53″	37°26′12″	85	24,307	688.870	262.74	9.94	3.78	235	310	2744
67. Palmeira dos Índios	9°24′58″	36°37′52″	296	73,337	450.990	263.04	9.88	3.76	236	304	2710
91. São Luís do Quitunde	09°19′06″	35°33′40″	4	34,825	397.257	263.66	9.93	3.77	236	311	2686
47. Maceió	9°39′59″	35°44′6″	4	1025,000	509.600	263.66	9.93	3.77	236	311	2686

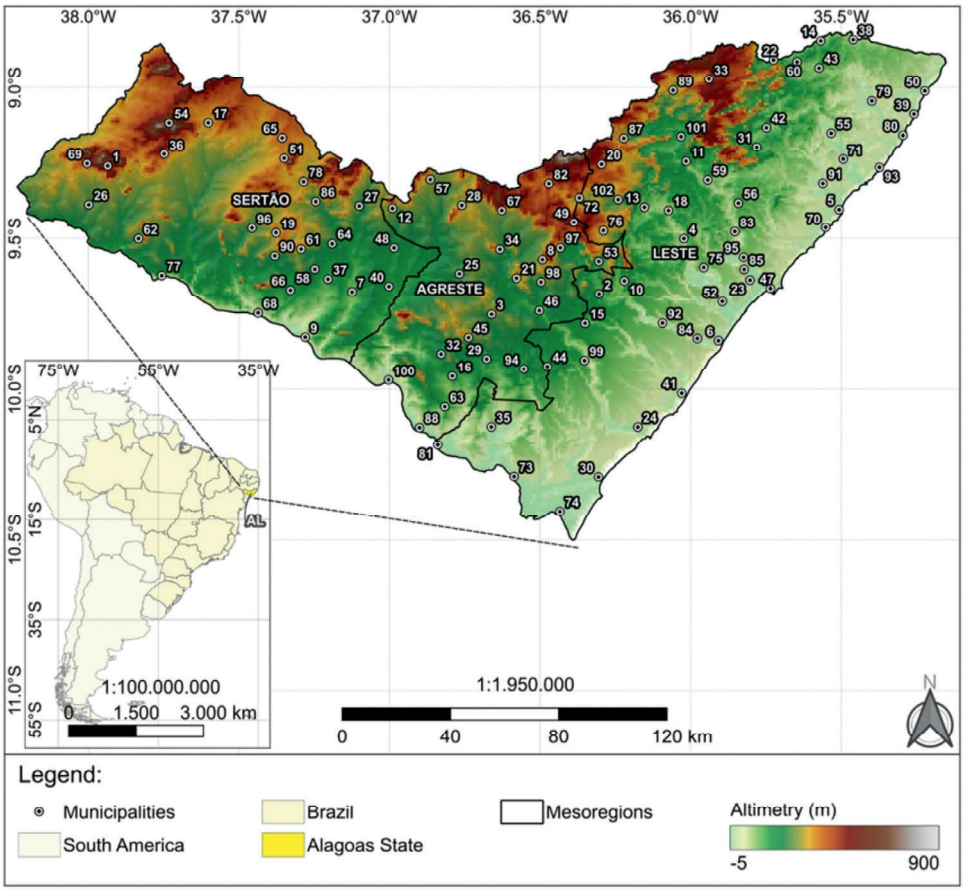

Fig. 1. Locations and altitudes (m) of automatic weather stations in Alagoas.

proaches employ neural networks and multivariate regression to improve the accuracy of TCO recovery, combining multiple spectral channels from sensors such as OMI, TROPOMI and GOME-2. The use of these algorithms increases the transparency and replicability of the study, allowing comparisons with global data and cross-validation with in situ measurements. In addition, these techniques are essential for detecting long-term trends and for assessing the impact of environmental policies, such as the Montreal Protocol, on the recovery of the ozone layer.

2.2. Data processing and statistical analysis

SISAM, launched in 2008, is a collaboration between Fiocruz, INPE, the Ministry of Health, and PAHO/WHO.This online platform makes it possible to assess exposure to air pollutants and its impact on human respiratory system by providing not only recent data on estimated air pollution concentrations, urban and industrial pollution, but also the monitoring of fire outbreaks and retroactive weather data between 2000 and 2019 for all municipalities in Brazil. In SISAM, all ten satellites equipped with orbital sensors in the 4μm thermal band are used. This data is processed by the DGI and Satellite Systems Division using imagery from polar satellites like AVHRR/3 (NOAA-18/19), Metop-B/C, NASA AQUA/TERRA, and VIIRS (NPP-Suomi, NOAA-20). Geostationary satellite images are also used, such as Aurea from the IMO sensor (INPE, 2019).

Despite its scope and technological sophistication, Sisam faces an important limitation: the lack of surface stations for data validation. The use of satellite data is valuable for providing a broad and continuous view of the environment, but this data has its inherent limitations and uncertainties. The installation of surface monitoring stations is essential to validate satellite data and improve the accuracy of analyses of the variability of the Total Ozone Column (TCO). Currently, several international and national initiatives promote the implementation of atmospheric monitoring networks. In Brazil, the National Environmental System (SISNAMA) and the National Institute for Space Research (INPE), through the Air Quality Monitoring System (SISAM), coordinate efforts to expand the network of measuring stations. In addition, programs such as the BREATHE Project, supported by the World Bank, encourage the creation of monitoring infrastructures in urban and vulnerable regions. At the international level, initiatives such as the Global Atmosphere Watch (GAW), of the World Meteorological Organization (WMO), and the Network for the Detection of Atmospheric Composition Change (NDACC) offer technical support and funding for continuous ozone monitoring projects. The European Union's Copernicus Programme and NASA's Health and Air Quality Applied Sciences Team (HAQAST) also provide data and support for air quality studies. To make this recommendation actionable in Alagoas, partnerships with universities and state environmental agencies, such as the Alagoas Environmental Institute (IMA-AL), can facilitate the installation of low-cost sensors for in-situ measurements, aligning with global monitoring guidelines and contributing to evidence-based public policies.

Although satellites provide data with wide spatial coverage, spatial resolution can be limited. This means that fine details, such as local variations in air pollution, cannot be captured accurately. Surface stations can provide detailed, localized measurements that complement satellite observations. Satellite data needs to be calibrated and validated with actual measurements to ensure that the observations are correct. Surface stations are essential to this val-

Table 2
Mann-Kendall trend test for the average annual ozone column concentrations (OCT) for the locations studied.

City	Annual		Summer		Autumn		Winter		Spring	
	Z	*p-value*	*Z*	*p-value*	*Z*	*p-value*	*Z*	*p-value*	*Z*	*p-value*
Arapiraca	2.12	0.03*	−0.85	0.39	−2.07	0.04*	2.52	0.01*	−0.50	0.62
Coruripe	1.75	0.08	−0.19	0.85	−2.57	0.01*	1.95	0.05	−1.00	0.31
Pão de Acucar	1.94	0.05	−0.66	0.51	−2.26	0.02*	1.77	0.08	−0.41	0.68
Palmeiras dos Índios	2.12	0.03*	−0.85	0.39	−2.07	0.04*	2.52	0.01*	−0.50	0.62
São Luis do Quitunde	2.84	0.01*	−0.26	0.80	−1.49	0.14	2.95	0.00*	−0.50	0.62
Maceió	2.79	0.01*	−0.26	0.80	−1.49	0.14	2.95	0.00*	−0.50	0.62

* - Significant at the level of 5%.

idation process, providing a reliable point of comparison. Surface stations can provide a continuous history of data at a fixed point, which is crucial for long-term studies and trend detection. Satellites, while comprehensive, may have gaps in data due to technical or orbital issues. Some satellite technologies may have difficulty distinguishing between different types of pollutants or their specific concentrations. Surface stations, equipped with specific instruments, can provide more detailed data on the composition of pollutants.

Therefore, to maximize the effectiveness of SISAM and ensure that it can provide highly reliable and usable data for public health and environmental policy, it is critical to invest in the installation and maintenance of a comprehensive network of surface monitoring stations. These stations would validate satellite data and offer essential information for a more accurate assessment of air quality and health impacts.

2.3. Applied statistics

Ozone data were analyzed using descriptive statistics (mean, max, min, CV%, SD), boxplots, homogeneity tests, and Mann-Kendall trend analysis (CMK) (Table 2). All analyses were done in R version 3.4.3 (R Core Team, 2021). For the analysis of the distribution functions, the following distributions were used: normal (or Gaussian) distribution, lognormal distribution, logistic distribution and Weibull distribution, and to know which is the best function that fits the data, the Kolmogorov-Smirnov test was used.

2.3.1. Normal (or gaussian) distribution

(1) Density function:

$$f(x) = \frac{1}{\sqrt{2\pi\sigma^2}} exp\left(-\frac{(x-\mu)^2}{2\sigma^2}\right) \quad (1)$$

where μ is the average of the distribution; σ^2 is variance.

(2) Features: Symmetrical around the mean μ. The distribution is characterized by its mean and variance. The shape of the distribution is a bell, known as the "bell-shaped curve" or "normal curve."

(3) Applications: Modeling of continuous variables that are symmetrically distributed around the mean. Used in statistics for inferences and hypothesis testing.

2.3.2. Lognormal distribution

(1) Density function:

$$f(x) = \frac{1}{x\sigma\sqrt{2\pi}} exp\left(-\frac{\left(lnx-\mu\right)^2}{2\sigma^2}\right) \quad (2)$$

where μ and σ^2 are the parameters of the normal distribution of the logarithm of the random variable.

(2) Features: Asymmetrical with a long tail on the right. The variable x has a lognormal distribution if lnx follows a normal distribution.

(3) Applications: Modeling data that is the product of many multiplicative factors, such as particle sizes, financial returns, and equipment lifetimes.

2.3.3. Logistic distribution

(1) Density function:

$$f(x) = \frac{exp\left(-\frac{(x-\mu)}{s}\right)}{s\left[1+exp\left(-\frac{(x-\mu)}{s}\right)\right]^2} \quad (3)$$

where μ is the location parameter (average), s is the scale parameter.

(2) Features: Logistic distribution is similar to the normal distribution, but with heavier tails. The cumulative distribution function (CDF) is a sigmoidal function.

(3) Applications: Used in logistic regression models and in analyses where growth or response is sigmoidal.

2.3.4. Weibull distribution

(1) Density function:

$$f(x) = \frac{\beta}{\eta}\left(\frac{x}{\eta}\right)^{\beta-1} \exp\left(-\left(\frac{x}{\eta}\right)^{\beta}\right) \quad (4)$$

where η is the scale parameter. β is the shape parameter.

(2) Features: You can model failure times with different patterns depending on the β value. $\beta < 1$ – decreasing failure rate; $\beta = 1$: constant failure rate (similar to the exponential distribution). $\beta > 1$: increasing failure rate.

(3) Applications: Survivability and reliability analysis, product life modeling, and time to failure.

2.3.5. Kolmogorov-Smirnov (K-S) test

(1) Objective: Compare an empirical distribution with a theoretical distribution or compare two empirical distributions to verify adequacy.

(2) Test statistic: The test calculates the maximum absolute difference between the empirical and theoretical distribution functions (or between two empirical distributions).

(3) Formula:

$$D = sup[F_n(x) - F(x)] \quad (5)$$

where $F_n(x)$ is the empirical distribution function. $F(x)$ is the theoretical distribution function.

(4) Features: The test is nonparametric and does not require assumptions about the shape of the theoretical distribution. The value of D is compared with critical values in a table to determine if the difference is statistically significant.

(5) Applications: Verification of data compliance with a theoretical distribution. Comparison of two samples to verify that they come from the same distribution.

These distributions and the Kolmogorov-Smirnov test are important tools in statistics and data analysis, each with its own characteristics and practical applications.

3. Results

The homogeneity test for the annual TCO and seasonal time series in Alagoas was conducted using the Bartlett test (1937) at 95% significance. The results indicated that the average annual and seasonal TCO values are homogeneous for all the series analyzed. Bartlett's test checks the homogeneity of variances across groups, testing the null hypothesis that all variances are equal against the alternative that at least one is different. This test is particularly relevant in analyses such as ANOVA, where the assumption of equal variances (homoscedasticity) is essential for the validity of the results. However, it is important to note that the Bartlett test is sensitive to the normality of the data; If the data does not follow a normal distribution, the test may erroneously indicate that the variances are different.

Table 1 presents the position and statistical dispersion of TCO concentrations in the analyzed municipalities. The annual average of TCO in the region is 263.24 ± 9.91 DU (Dobson Units), with a maximum value of 311 DU observed in the cities of Maceió and São Luís do Quitunde, and a minimum value of 304 DU in Arapiraca. When analyzing the annual averages of TCO, it was considered essential to assess the degree of dispersion of these data. The standard deviation (σ), indicating data uniformity (Wilks, 2006), averaged 9.91 DU, with a maximum of 9.94 DU and a minimum of 9.87 DU across cities. The average coefficient of variation was 3.77%, with a maximum of 3.78% and a minimum of 3.75%, indicating a low variation and suggesting that the regions studied have homogeneous characteristics. TCO distribution homogeneity is linked to regional factors like the Brewer-Dobson Circulation (CBD), which is minimally affected by the weak Antarctic Polar Vortex (VPA) in this area (Hauchecorne et al., 2002; Solomon et al., 2016).This atmospheric dynamic facilitates the uniform distribution of observed ozone concentrations.

From an environmental and public health perspective, variations in TCO concentration can have significant impacts. Stratospheric ozone concentration is vital for protecting life on Earth from harmful ultraviolet (UV) rays. Therefore, homogeneity in the distribution of the ozone suggests a relatively uniform protection against UV radiation in Alagoas, which is positive for public health. On the other hand, any significant variation in TCO may indicate changes in atmospheric conditions that could lead to adverse consequences, such as increased risk of skin cancer and other health problems related to UV radiation exposure. Additionally, TCO analysis can provide important insights into climate change and atmospheric circulation patterns, which are key to understanding large-scale environmental changes. Therefore, ongoing studies on TCO and its variations are essential to monitor environmental impacts and protect public health.

3.1. Contextual mann-kendall contextual (CMK) method

The Contextual Mann-Kendall (CMK) method was used to analyze the trends of the temporal data. This method is an extension of the Mann-Kendall test, which is widely used to detect trends in hydrological and climatic time series.

Specific steps include

(1) Data collection and pre-processing: The data were collected from reliable sources and organized into time series. Data cleansing was performed to remove anomalous values and address potential gaps in the time series. The data were normalized to ensure comparability between different data sets.
(2) Application of the CMK method: The time series were divided into movable windows for contextual analysis. In each window, the Kendall coefficient was calculated to detect the presence of monotonic trends. Statistical significance analysis was performed to determine the reliability of the observed trends.
(3) Interpretation of the results: Trends detected in different windows were compared to identify temporal and spatial patterns. The trends were classified according to their magnitude and significance.

All statistical analyses were performed in the R environment version 3.4.3 (R Core Team, 2021). R is a programming language that is widely used for statistical analysis and data manipulation. R-specific packages used include: trend: to run the Mann-Kendall test and its contextual variations.

Zoo: to manipulate time series.

DPLYR: for data cleansing and transformation. ggplot2: for graphical visualization of the results.

The pre-processing of the data included the following steps:

Data Cleansing: Removal of missing values and outliers using dplyr package functions.

Normalization: Applying normalization techniques to standardize data, ensuring that different units were comparable.

Moving window splitting: Using the zoo package to create moving windows in the time series, making contextual analysis easier.

The analysis of Table 2, which presents the results of the Mann-Kendall trend test for the average annual and seasonal total ozone column (TCO) concentrations in the studied cities, can be interpreted as follows:

(1) Annual trend

All cities have positive ***Z*** values, indicating an increasing trend in TCO over the years.

The cities Arapiraca, Palmeiras dos Índios, São Luís do Quitunde, and Maceió show statistically significant trends ($p\text{-}value < 0.05$). This suggests a consistent increase in the annual average ozone concentration in these locations.

(2) Summer trend

All cities have negative ***Z*** values, but the *p-values* are high (>0.05), indicating no significant trend in summer.

(3) Autumn trend

All cities show negative ***Z*** values, indicating a decreasing trend in TCO during this season. In Arapiraca, Coruripe, and Pão de Açúcar, this decreasing trend is statistically significant ($p\text{-}value < 0.05$).

(4) Winter Trend

Z values are positive for all cities, suggesting an increasing trend in TCO during winter.

This trend is statistically significant in Arapiraca, Palmeiras dos Índios, São Luís do Quitunde, and Maceió.

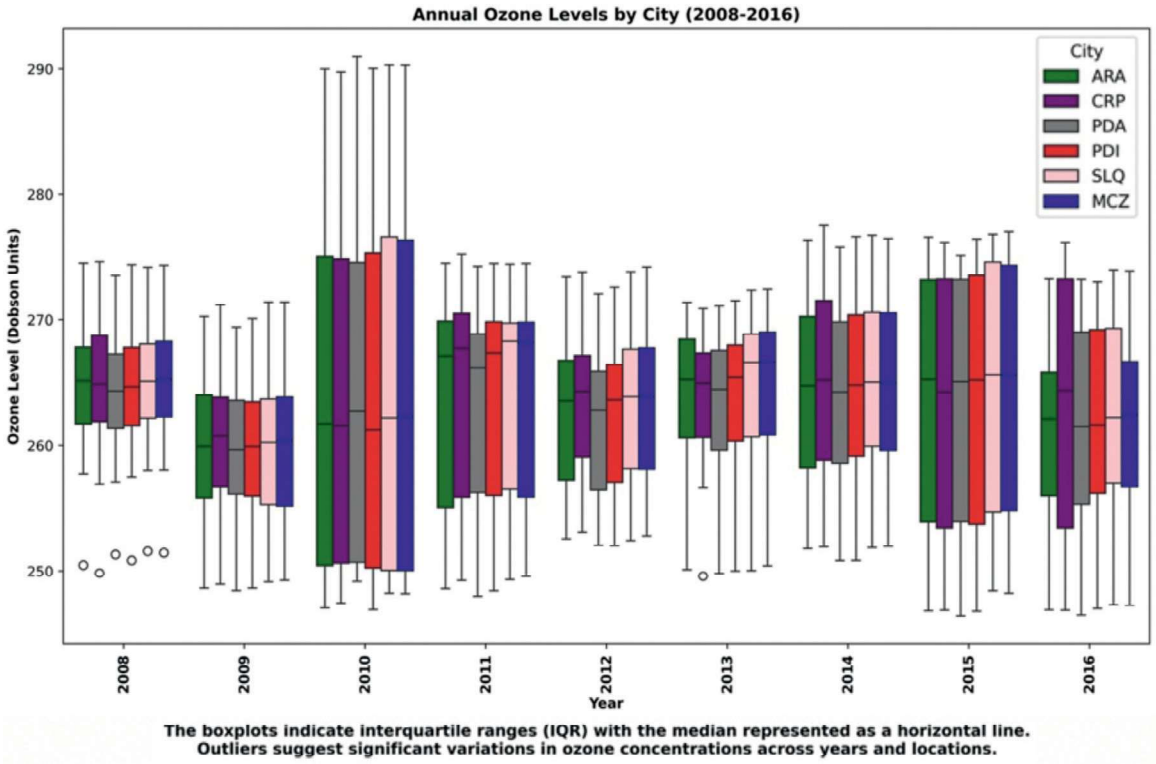

Fig. 2. Boxplot showing annual ozone levels (Dobson Units) for six cities from 2008 to 2016. The boxplots indicate interquartile ranges (IQR) with the median represented as a horizontal line. Outliers suggest significant variations in ozone concentrations across years and locations.

(5) Spring trend

Z values are mixed, but all *p-values* are high (>0.05), indicating no significant trends during this season. There is a significant increasing trend in TCO over the years in some cities, particularly Arapiraca, Palmeiras dos Índios, São Luís do Quitunde, and Maceió. The decreasing trend in TCO during autumn is significant in some locations, possibly reflecting seasonal atmospheric circulation patterns.

Winter shows a significant increasing trend in some cities, which may be related to meteorological factors and regional atmospheric dynamics. No significant trends were observed in summer and spring.

Fig. 2 illustrates the average monthly TCO in DU in the six cities from 2008 to 2016. Maceió and São Luiz do Quitunde recorded the highest TCO values at 263.66 ± 9.93 DU, with São Luiz do Quitunde reaching a maximum of 311 DU. Pão de Açúcar recorded the lowest TCO at 235 DU, with a variation of 76 DU. In contrast, Souza et al. (2022a) reported ozone concentrations in Mato Grosso do Sul from 2005 to 2020 ranged from 260 DU in the Pantanal to 347 DU in the Cerrado, with a 101 DU variation.

The analysis highlights temporal and seasonal fluctuations in ozone concentrations, reaching the peak on 09/13/2010 (winter) for the cities of São L do Quintude and Maceió (311 DU); 09/13/2010 (winter) for the cities of Arapiraca (304 DU), Coruripe (319) and Palmeira dos Índios (304 DU) and Pão de Açúcar on 10/22/2010 (winter) with (310 DU). In the seasons of the year, the highest average TCO occurs in the spring season with an average of 271 DU. This seasonality underscores the profound influence of climatic and seasonal factors on ozone dynamics, emphasizing its critical role in interpreting atmospheric trends. These findings deepen our understanding of ozone distribution and the impact of seasonal and climate variations, for effective environmental management and strategies to mitigate potential impacts on regional air quality. The homogeneous distribution of TCO according to research (Hauchecorne et al. 2002; Solomon et al. 2016), can be attributed to the Brewer-Dobson Circulation (CBD), which does not suffer significant interference from the Antarctic Polar Vortex (VPA), which, in this region, has a weak intensity. This atmospheric dynamic contributes to the uniform distribution of observed ozone concentrations.

Crespo et al. (2011) reported a decline in total ozone over southern Brazil from 1979 to 1996. A 7.0 ± 2.9 DU reduction occurred in 62 events from 2005 to 2014. These events were more frequent in October, the positive phase of the ENSO index had a significant influence on most events, while the QBO showed a balance in its influence. These findings underscore the importance of understanding the interplay between global and regional phenomena on ozone variability.

In Alagoas (2008–2017), minimum ozone values dropped by 5% per year in May. The Mann-Kendall analysis showed a slight increase in tropospheric ozone (1.75–2.84 DU) and a seasonal decrease in stratospheric ozone, except for an increase in winter. Significant annual trends were found in several cities, linked to ozone precursor emissions from anthropogenic activities like urbanization, transportation, and biomass burning. These results align with studies noting the impact of biomass burning on ozone, especially during spring (Clain et al., 2009; Thompson et al., 2014; Souza et al., 2022).

The decrease in the TOC in the region can be explained by several factors that interact in a complex way in the atmosphere: The Brewer-Dobson Circulation (BDC) is an atmospheric process that transports ozone from the tropical region to the poles. Changes in the intensity and structure of this circulation can influence the amount of ozone that remains in tropical regions, including the region. During certain weather phenomena, such as El Niño, this circulation can be altered, reducing the amount of ozone transported to tropical areas. El Niño and QBO are phenomena that affect the distribution of ozone in the stratosphere and troposphere. During

Table 3
Variations in the Total Ozone (TCO) average column in the periods associated with El Niño, La Niña and neutral conditions for the cities analyzed.

	Arapiraca	Coruruipe	Pão Açucar	Palmeiras Índios	S L Quitunde	Maceió
El Niño (anomalous warming in the Equatorial Pacific):						
2009–2010	262.03	262.40	262.34	262.03	262.56	262.56
2014–2016	263.12	263.31	262.75	263.12	263.76	263.76
La Niña (anomalous cooling in the Equatorial Pacific):						
2007–2008	264.47	264.26	264.09	264.47	264.88	264.88
2010–2011	262.95	263.17	262.80	262.95	263.42	263.42
2011–2012	262.66	263.58	262.05	262.66	263.35	263.35
Neutral (absence of significant El Niño or La Niña):						
2008–2009	262.35	262.52	261.97	262.35	262.72	262.72
2012–2013	262.93	263.44	262.44	262.93	263.84	263.84
2013–2014	264.16	264.46	263.66	264.16	264.84	264.84

El Niño events, for example, changes in atmospheric circulation can lead to a temporary reduction in ozone concentrations in certain regions. These variations are caused by changes in wind patterns and the temperature of the stratosphere. The seasonal cycle of ozone can vary, with lower concentrations observed at certain times of the year due to natural changes in atmospheric dynamics. In tropical regions, ozone levels can vary due to semiannual modes and local pollutants, despite reductions in ozone-depleting substances under the Montreal Protocol. Residual effects and pollutant interactions may cause temporary declines in the Total Ozone Column, increasing UV exposure risks. These findings highlight the need for continuous monitoring to support effective environmental management and policymaking.

The interannual and seasonal variability of the TCO from 2008 to 2016 shows values typically between 304 and 311 DU, with an atypical peak in 2010, consistent with earlier studies (Sousa et al. 2020a). The TCO varies smoothly, with a minimum of 250 DU in May and a maximum of 274 DU in October. Early-year values remain stable around 262–263 DU, decreasing until May and then rising until October, followed by a gradual decline in November and December. This annual cycle aligns with findings from Dias Nunes (2017, 2020). Normal, Lognormal, Logistic, and Weibull PDFs were applied to model the TCO from 2008 to 2016. These distributions are common in environmental studies to analyze variables like ozone. The Kolmogorov-Smirnov (KS) test was used to evaluate the best fit, with the Normal distribution providing the closest match (p-value $>$ 0.05). Asymmetry analysis of the distributions for each city showed good alignment between the estimated and empirical data. A similar study by Souza et al. (2020b) used 15 PDFs to analyze ozone concentrations and seasonal variations in Campo Grande, Brazil.

The distributions were evaluated using KS, AD, and Chi-Square tests. The comparative analysis of the results indicated that the generalized distribution of extreme values provided a good overall adjustment throughout the year. However, specific stations showed variations in the best-fit distributions. For winter, the 3-parameter Gamma distribution was the most suitable, while the 3-parameter Lognormal distribution adjusted better in the spring, and the Weibull distribution was optimal for the summer. Autumn showed a good fit with the 3-parameter Gamma distribution. Both autumn and winter, with lower O_3 levels, kurtosis, and asymmetry, had similar distribution fits. On the other hand, summer and spring, marked by higher O_3 concentrations and different kurtosis and asymmetry values, required distinct PDFs (Tables 3, 4, 5 and Fig. 3).

A negative slope from 2008 to 2009 indicates a temporary TCO decrease, followed by a gradual rise. This trend in Alagoas may not reflect broader regional or global patterns. Further investigation into the causes of these TCO fluctuations, such as changes in atmospheric circulation patterns, anthropogenic emissions, or natural phenomena, would provide valuable insights into their underlying mechanisms and implications for ozone layer protection. The interannual variability of TCO is predominantly influenced by annual variations in local weather, solar activity, teleconnection patterns, and other weather modes. Solar radiation affects ozone concentrations through photochemical reactions and influences atmospheric circulation and ozone distribution in the stratosphere. These interannual variations also coincide with ENSO events, in which TCO tends to increase during El Niño years: 2009–2010 (+4 DU or 1.54%, 2014–2016 (3 DU or 1.13%); La Niña: 2008–2009 (−5DU or (1.89%), 2010–2011 (zero), 2011–2012 (−1 or 0.38%), 2016–2017 (−2 DU or 0.76%). Cyclical events vary in intensity, with some stronger than others. Studies show complex TCO variations. Significant negative trends in January, indicate potential ozone declines, while mixed trends across seasons and latitudes appear due to differing methodologies and conditions. In addition, Further complexity by examining the Hindu Kush Himalayan and Tien Shan regions, revealing significant seasonal variations with predominantly negative trends in summer and autumn, contrasting with positive trends in winter. These findings highlight the seasonal variability in ozone behavior influenced by local climatic conditions and interactions with other factors. In conclusion, these studies underscore the complexity of TCO trends and emphasize the importance

Table 4
Maximum likelihood estimates of the parameters. Please check the parameters.

City	Normal		Lognormal		Logistic		Weibull	
	μ	σ	μ	σ	μ	s	η	β
Arapiraca	263.041	9.881	263.041	9.868	262.986	10.371	26.111	267.843
Coruripe	263.364	9.894	263.364	9.889	263.371	10.391	26.0835	268.141
Pão de Acucar	262.742	9.938	262.741	9.9098	262.640	10.357	24.928	267.588
Palmeiras dos Índios	263.041	9.881	263.041	9.868	262.986	10.371	26.111	267.843
São Luís do Quitunde	263.664	9.93084	263.664	9.9176	263.629	10.4231	25.5917	268.473
Maceió	263.664	9.93084	263.664	9.9176	263.629	10.4231	25.5917	268.473

Table 5
The results of the Kolmogorov-Smirnov test for the cities considered.

City	Normal *KS*	Lognormal *KS*	Logistic *KS*	Weibull *KS*
Arapiraca	0.0359810	0.0425622	0.0458058	0.0766897
Coruripe	0.0419108	0.0486879	0.049653	0.0747125
Pão deAcucar	0.0356803	0.0369833	0.0450819	0.0864402
Palmeiras dos Índios	0.0359810	0.0425622	0.0458058	0.0766897
São Luís do Quitunde	0.0382296	0.0442023	0.0494535	0.0797962
Maceió	0.0382296	0.0442023	0.0494535	0.0797962

of integrated, long-term monitoring and research to fully understand regional atmospheric and climate changes.

Fig. 4 illustrates the monthly average changes in TCO for the region. The highest average TCO of 275 DU was recorded in September in Maceió, while the lowest average of 250 DU occurred in May in Coruripe. Data analysis, along with comparisons (Sousa et al., 2020b), indicates that the annual cycle predominates seasonal TCO variability, driven by changes in solar radiation and atmospheric temperature, leading to higher ozone concentrations in September and lower in May.

Fig. 5 presents the seasonal variation of interannual averages of Total Ozone Column (TCO) for the region. The highest average TCO of 283 DU was observed in spring (OND – October to December) at the Coruripe station, while the lowest average of 249 DU occurred in fall (AMJ – April to June). The analysis emphasizes the importance of data dispersion, with standard deviation (SD) indicating variability. The data reveals a mid-latitude seasonal pattern, with minimal TCO variability from April to June and August to September, while transition months (January, February, July, October to December) show greater variability around ±7.6 DU.

The seasonal cycle indicates that after spring, winter and summer have intermediate TCO levels, while autumn consistently records the lowest values. This regular pattern, characterized by a single annual peak and minimum, mirrors trends observed at mid- and high latitudes. Notably, equatorial regions show a much lower TCO amplitude (∼24 DU) compared to the 76 DU variability in the studied region. Seasonal ozone variability in this region is influenced by atmospheric circulation, local weather, and human activities. TCO peaks in September/October and dips in May, reflecting mid-latitude patterns. Variations across latitudes result from large-scale circulation redistributing air masses. Understanding these changes is crucial for assessing air quality and informing environmental policies aimed at reducing emissions and promoting sustainable development goals (SDGs). Continuous monitoring is essential for evaluating the impacts of human activities and climate change on air quality. Figs. 5a, 5b, and 6 illustrate the spatial distribution of seasonal monthly average TOC from the OMI sensor on the Aura satellite during 2008–2016, showing the largest distribution in spring (OND) and the smallest in autumn (AMJ), consistent with Fig. 5.

The average annual TCO value evaluated from 2008 to 2016 was 263.50 ± 1.51 DU, reaching a maximum of 264.04 ± 1.75 DU and a minimum of 268.89 ± 1.46 DU (Table 1). Specifically, the highest monthly average occurred in 2010 in the municipality of Arapiraca, measuring 266.07 DU, while the lowest was recorded in 2015 in the municipality of Palmeira dos Índios with 261.80 DU (Fig. 6a). Over the years, the monthly average TCO fluctuated around 263.50 ± 0.40 DU, with a maximum of 274.56 ± 0.45 DU and a minimum of 250.09 ± 0.35 DU. October recorded the highest average of 275.08 DU in Coruripe, while May had the lowest at 249.66 DU in Palmeira dos Índios. The low May value is linked to the winter solstice, while higher values in October/November correspond to the sun's zenith and reduced cloud cover. Interannual TCO behaviors were notably similar across the six study regions.

Seasonal analysis of the O_3 data reveals distinct variations in concentration and variability at different altitudes and seasons (Figs. 5 and 6). The results indicate TCO peaks during the spring (OND – October, November, and December) and lows during the fall (AMJ – April, May, and June). This cyclical behavior is closely related to the Earth's position in its orbit around the Sun, where solar radiation influences the production of ozone in the stratosphere, resulting in two maximums and two minimums throughout the year. (Fig. 5).

3.2. Variation of TCO during El Niño, La Niña and Neutral periods

Table 3 presents the variations in Total Column Ozone (TCO) during periods associated with El Niño, La Niña, and neutral conditions for the analyzed cities. The analysis of TCO for cities in Mato Grosso do Sul during El Niño, La Niña, and neutral periods reveals distinct patterns in tropospheric ozone variability.

(1) El Niño (2009–2010, 2014–2016)

During El Niño events, average TCO values were slightly lower compared to netral and La Niña periods. This behavior may be associated with the anomalous warming of Pacific Equatorial waters, which influences global atmospheric circulation and may reduce ozone transport to the stratosphere. Notably, the average TCO values in 2014–2016 were slightly higher than in 2009–2010, possibly due to differences in the intensity of the El Niño phenomenon between the analyzed periods.

(2) La Niña (2007–2008, 2010–2012)

During La Niña, TCO values were higher than those recorded during El Niño and neutral periods. The anomalous cooling of Pacific waters favors atmospheric circulation that enhances ozone transport to the stratosphere, resulting in higher concentrations. The 2007–2008 period exhibited the highest average TCO values, suggesting that atmospheric conditions favored greater retention and redistribution of ozone in the region.

(3) Neutral periods (2008–2009, 2012–2014)

During neutral periods, TCO values were intermediate, without significant extreme variations. This stability is consistent with the absence of major climatic drivers such as El Niño or La Niña, leading to normal atmospheric circulation patterns. However, minor variations may occur due to local factors, such as seasonal patterns and interannual variability.

The relationship between the El Niño-Southern Oscillation (ENSO) and TCO variability indicates that La Niña events tend to increase ozone concentrations, while El Niño events may reduce them. This influence highlights the importance of considering global climatic factors when analyzing ozone variability in the region. Further studies could explore the relationship between ENSO intensity and seasonal TCO patterns, contributing to a better understanding of atmospheric dynamics.

4. Discussion

4.1. The analysis of the TCO

Data in six cities in the Alagoas region revealed significant seasonal patterns, providing new insights into local atmospheric dynamics. This study identified a dominant biannual cycle in the seasonal variability of TCO, a phenomenon that had not been widely discussed in the current literature.

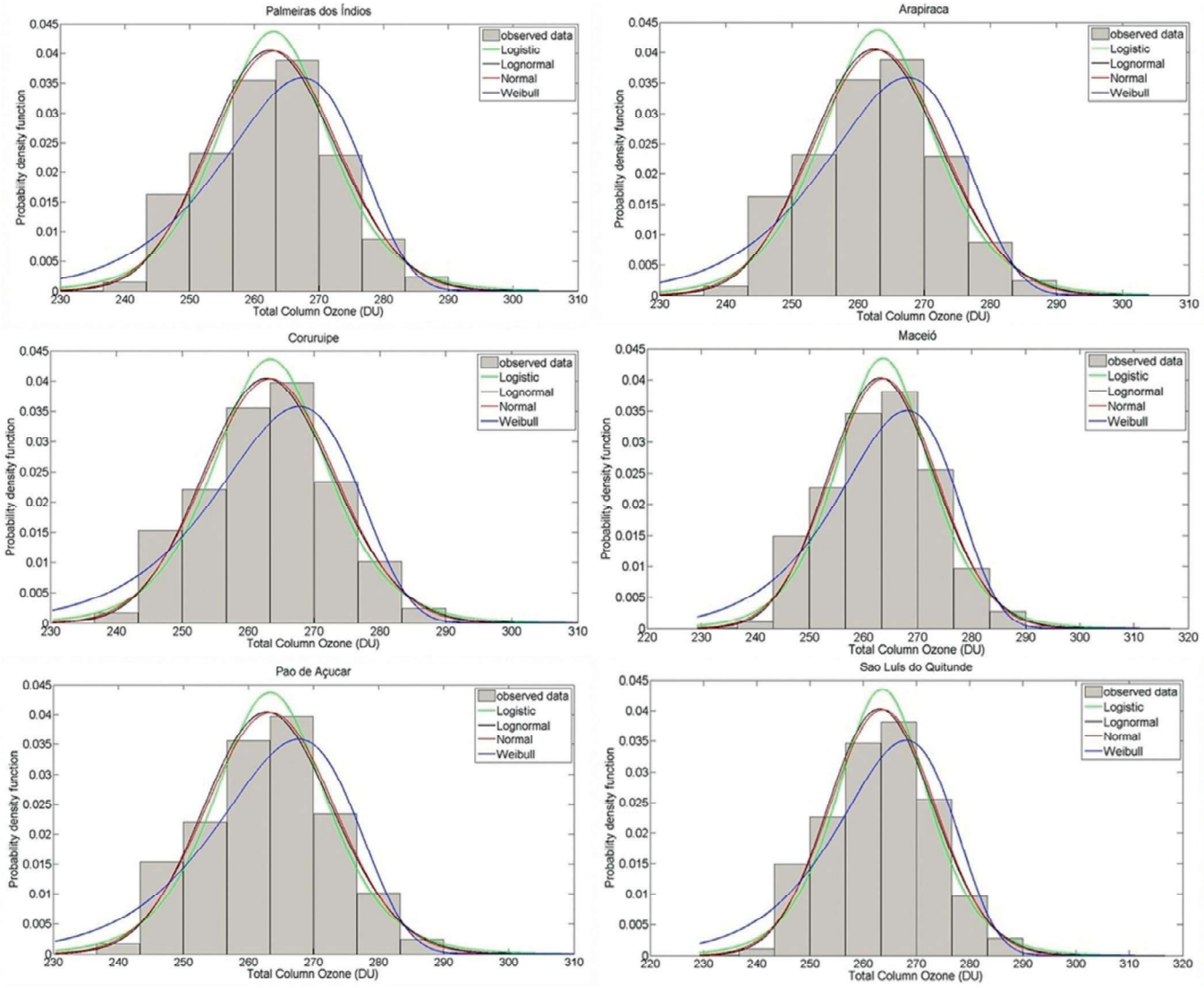

Fig. 3. The logistic, lognormal, normal, and Weibull histograms and PDFs adjusted for the TCO data over a 9-year period (2008–2016) for all six cities in the study.

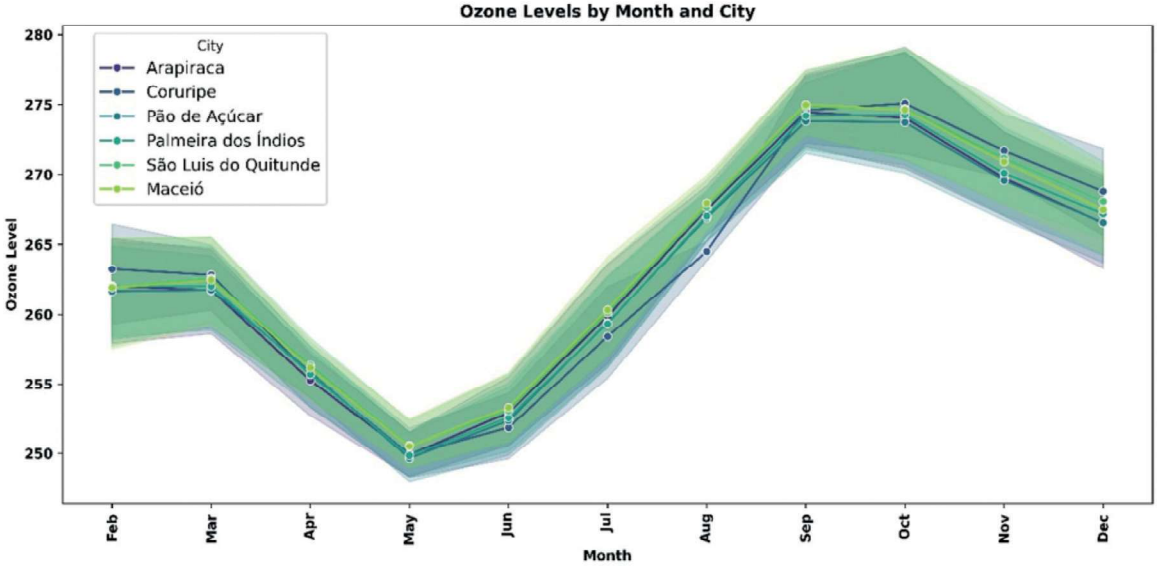

Fig. 4. Interannual seasonal time series (year stickers) of TCO in DU in the region for the period (2008–2016) obtained from the OMI sensor on the aura satellite.

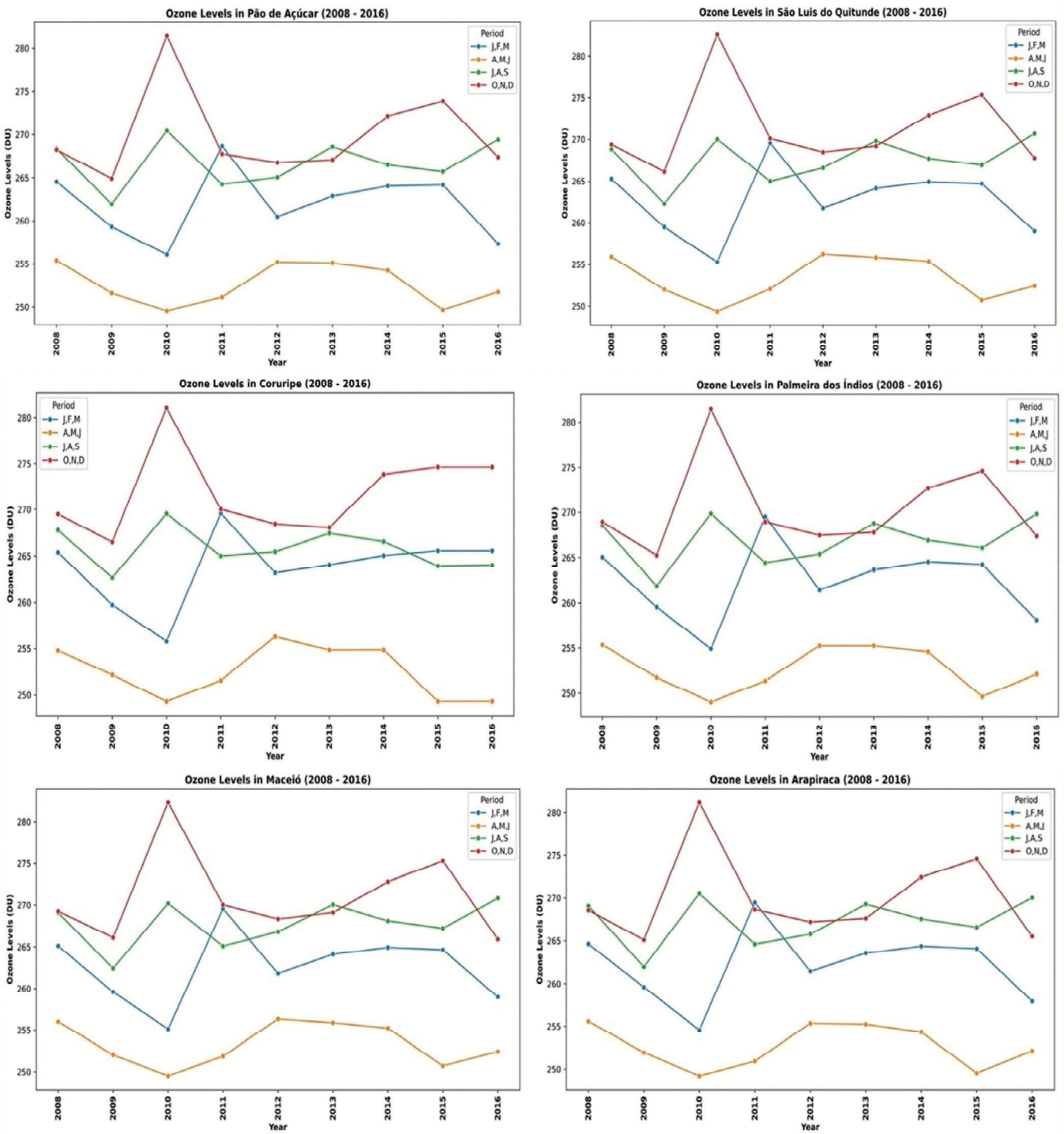

Fig. 5. (a) Average change in TCO in the region in the period (2008–2016). (b) Average change in TCO in the region in the period (2008–2016) by year.

The annual ozone cycle is closely tied to the Earth's orbit around the Sun, affecting solar radiation intensity and, in turn, ozone production and destruction in the stratosphere. Increased UV radiation during spring enhances the dissociation of O_2 into O atoms, leading to peak ozone levels. Conversely, autumn's reduced UV radiation and lower temperatures contribute to decreased ozone production and greater depletion, resulting in minimum levels.

This cycle features two peaks in spring and a smaller one in fall, with lows typically occurring in autumn and winter. The findings show TCO peaks during spring (OND – October, November, December) and lows in fall (AMJ – April, May, June), consistent with seasonal variations observed in mid-latitude regions by Xie et al. (2014a, 2014b). In regional terms, coastal cities, such as Maceió and Coruripe, had the highest seasonal averages of TCO, especially during the spring. This can be attributed to the higher intensity of solar radiation and the influence of sea currents, which can affect local atmospheric circulation. In contrast, inland cities, such as Palmeira dos Índios, showed less variability in TCO, suggesting more stable atmospheric conditions. Compared with previous studies, such as those by Lima et al. (2020, 2021), which also observed seasonal patterns in other mid-latitude regions, the findings of this

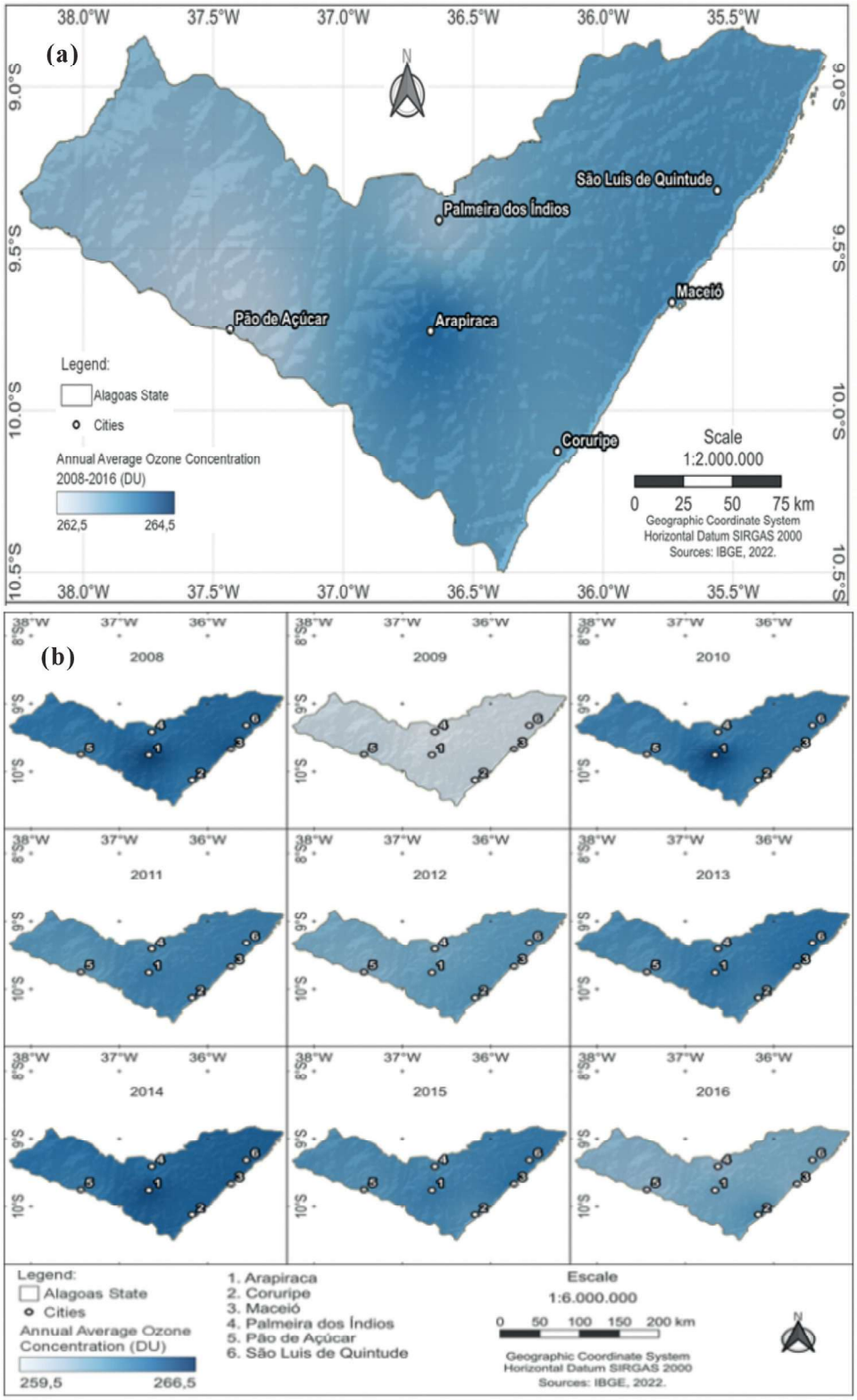

Fig. 6. Average change in TCO in the region for the period (2008–2016) by month.

study provide a new perspective by highlighting the dominance of the biannual cycle in the Alagoas region. This finding suggests the need to reevaluate theories about ozone dynamics in tropical regions. In addition to contributing to scientific understanding, seasonal variations in TCO have practical implications for air quality and environmental policymaking in the region. Understanding these patterns can inform strategies for mitigating the effects of climate change and help develop more effective public health policies.

Regarding the possible limitations of the study, the TCO data were obtained from satellites, which may represent a limitation due to the restricted temporal and spatial coverage. Insufficiently

long observation periods or limited spatial data may affect the representativeness of the results. The accuracy of TCO data can also be influenced by factors such as the resolution of the measuring instruments, calibration errors, or atmospheric interference. The lack of complementary data, such as detailed meteorological information, may limit the interpretation of the mechanisms underlying the observed variations in TCO. In addition, the choice of statistical methods used to analyze the variation in TCO can influence the results, and alternative or more advanced methods could provide different insights. Analyses performed on monthly, annual, and seasonal averages can mask diurnal variability or extreme events that are important for a full understanding of ozone dynamics. It is possible that the results indicate correlations, but without proving direct causality between the variables analyzed and the variations in TCO. Generalizing the results to different contexts or periods can be challenging, especially if the study was conducted under specific environmental or social conditions. Comparing results with the existing literature may be limited if the studies being compared were conducted under significantly different environmental, temporal, or methodological conditions.

The study of the seasonal dynamics of TCO and its connection to global climate events, such as ENSO, provides a solid basis for informing public policies aimed at public health and environmental management. In addition to protecting the health of the population through UV mitigation strategies, the findings can also contribute to actions to reduce air pollutants, adapt agriculture and strengthen urban infrastructure to face global climate challenges. These policies can be flexible and dynamic, adjusting according to TCO variations and the needs of the local population.

5. Conclusions

This study examined the seasonal and interannual variability of the Total Ozone Column (TCO) in six cities in Alagoas, using satellite data and statistical analyses. The results revealed a distinct seasonal pattern, with maximum TCO values in spring (October to December) and minimum values in autumn (April to June). This cycle is influenced by Earth's orbit around the Sun and the photochemistry of stratospheric ozone.

Additionally, a dominant biennial cycle was identified, showing two peaks and two troughs throughout the year, corresponding to the Sun's passage over the region. Notably, Coruripe exhibited the highest average TCO values, while Maceió recorded the lowest, highlighting the spatial variability within the region.

These findings provide valuable insights for air quality management and environmental policy development in Alagoas, particularly concerning exposure to UV radiation. Understanding ozone dynamics is essential to strengthening mitigation strategies for risks associated with ultraviolet radiation, including awareness campaigns on sun protection and continuous ozone layer monitoring.

(1) Practical recommendations for air quality management:

(a) **Continuous TCO monitoring** – Installing complementary monitoring stations and incorporating satellite data can enhance the detection of seasonal variations and long-term trends, allowing for the formulation of preventive policies.
(b) **Integration with UV radiation alerts** – TCO variation directly impacts the levels of ultraviolet radiation reaching the surface. Developing alert systems for excessive UV exposure can reduce health impacts, especially for vulnerable populations.
(c) **Policies to reduce precursor pollutants** – Although this study focused on the stratosphere, the interaction between tropospheric and stratospheric ozone is critical. Implementing policies to reduce ozone precursor emissions (NOx and VOCs) can help improve air quality.
(d) **Development of predictive models** – Integrating statistical models and artificial intelligence can improve TCO variation forecasts, enabling more effective responses to extreme events, such as sudden increases in UV radiation.
(e) **Education and public campaigns** – Awareness efforts regarding the relationship between ozone and UV radiation can encourage the use of sunscreen, appropriate clothing, and safe sun exposure times.

(2) Alignment with global efforts:

The results of this study reinforce the importance of monitoring the ozone layer at a regional scale, complementing international initiatives such as the *Montreal Protocol* and atmospheric observation programs by the World Meteorological Organization (WMO) and the European Space Agency (ESA). Additionally, recent research indicates that ozone layer recovery is uneven across regions, with significant impacts in tropical areas. This study contributes to the understanding of these variations and provides insights for initiatives aimed at mitigating the effects of climate change on stratospheric ozone circulation.

Future research should further investigate the meteorological and anthropogenic factors affecting TCO and consider integrating advanced forecasting models to enhance analytical precision. Additionally, expanding the analysis to cover longer periods is recommended to assess long-term trends and the impacts of climate variability on the ozone layer in Brazil's northeastern region.

Declaration of competing interest

The authors declare that there are no conflicting interests.

CRediT authorship contribution statement

Amaury de Souza: Writing – review & editing, Writing – original draft, Conceptualization. **Celina M. Takemura:** Formal analysis, Data curation. **Deniz Özonur:** Formal analysis, Data curation, Conceptualization. **Elias Silva de Medeiros:** Resources, Project administration, Methodology. **Ivana Pobocikova:** Investigation, Funding acquisition, Conceptualization. **Janice F. Leivas:** Investigation, Funding acquisition. **José Francisco de Oliveira-Júnior:** Formal analysis, Data curation, Conceptualization. **Kelvy Rosalvo Alencar Cardoso:** Data curation, Conceptualization. **Marcel Carvalho Abreu:** Funding acquisition, Formal analysis. **Wagner Alessandro Pansera:** Validation, Software, Formal analysis. **Jose Roberto Zenteno Jimenez:** Formal analysis, Software, Validation. **Sneha Gautam:** Writing – review & editing, Writing – original draft, Supervision, Data curation, Conceptualization.

Data Availability

The data generated or analyzed during this study are presented in this article and can be accessed at .

Supplementary materials

Supplementary material associated with this article can be found, in the online version, at doi:10.1016/j.geogeo.2025.100379.

References

Albers, J.R., Perlwitz, J., Butler, A.H., Birner, T., Kiladis, G.N., Lawrence, Z.D., Manney, G.L., Langford, A.O., Dias, J., 2018. Mechanisms governing interannual variability of stratosphere-to-troposphere ozone transport. J. Geophys. Res. 123 (1), 234–260. doi:10.1002/2017JD027677.

Bartlett, M.S., 1937. Properties of sufficiency and statistical tests. In: Proceedings of the Royal Society of London. Series A, Mathematical and Physical Sciences, 160, pp. 268–282. doi:10.1098/rspa.1937.0109.

Braesicke, P., Neu, J., Fioletov, V., Godin-Beekmann, S., Hubert, D., Petropavlovskikh, I., Shiotani, M., Sinnhuber, B.-M., 2018. Update on global ozone: past, present, and future. Scientific Assessment of Ozone Depletion: 2018 (Report No. 58). Global Ozone Research and Monitoring Project – World Meteorological Organization. https://ozone.unep.org/sites/default/files/2019-05/SAP-2018-Assessment-report.pdf.

Clain, G., Baray, J.L., Delmas, R., Diab, R., Leclair de Bellevue, J., Keckhut, P., Posny, F., Metzger, J.M., Cammas, J.P., 2009. Tropospheric ozone climatology at two Southern Hemisphere tropical/subtropical sites (Reunion Island and Irene, South Africa) from ozone sondes, LIDAR, and in situ aircraft measurements. Atmos. Chem. Phys. 9, 1723–1734. doi:10.5194/acp-9-1723-2009.

Coldewey-Egbers, M., et al., 2022a. The global total ozone recovery as seen by multi-sensor reanalysis data. Atmos. Chem. Phys. 22, 13589–13608. doi:10.5194/acp-22-13589-2022.

Coldewey-Egbers, M., Loyola, D.G., Lerot, C., Van Roozendael, M., 2022b. Global, regional and seasonal analysis of total ozone trends derived from the 1995–2020 GTO-ECV climate data record. Atmos. Chem. Phys. 22, 6861–6878. doi:10.5194/acp-22-6861-2022.

Crespo, N.M., Leme, N.M.P., Veres, L.V., Kall, E., 2011. Average behavior of the total ozone column from 1992 to 2010 over the Southern Space Observatory. In: Proceedings of the 26th Integrated Academic Journey. UFSM, Santa Maria, Brazil, p. 1.

Diallo, M., Riese, M., Birner, T., Konopka, P., Müller, R., Hegglin, M.I., Santee, M.L., Baldwin, M., Legras, B., Ploeger, F., 2018. Response of stratospheric water vapor and ozone to the unusual timing of El Niño and the QBO disruption in 2015-2016. Atmos. Chem. Phys. 18 (17), 13055–13073. doi:10.5194/acp-18-13055-2018.

Dias Nunes, M., 2017. Influence of the Total Ozone Column On the Variability of Ultraviolet Radiation Over the South of South America (Master's Dissertation. Federal University of Pelotas), Pelotas.

Dias Nunes, M., Mariano, G.L., Alonso, M.F., 2020. Spatiotemporal variability of the total ozone column and its relationship with ultraviolet radiation in South America. Brazil. J. Phys. Geogr. 13 (5), 2053–2073. doi:10.26848/rbgf.v13.5.p2053-2073.

Gilford, D.M., Solomon, S., 2017. Radiative effects of stratospheric seasonal cycles in the tropical upper troposphere and lower stratosphere. J Clim 30 (8), 2769–2783. doi:10.1175/JCLI-D-16-0268.1.

Grise, K.M., Polvani, L.M., Tselioudis, G., Wu, Y., Zelinka, M.D., 2013. The ozone hole indirect effect: cloud-radiative anomalies accompanying the poleward shift of the eddy-driven jet in the Southern Hemisphere. Geophys. Res. Lett. 40 (14), 3688–3692. doi:10.1002/grl.50686.

Grise, K.M., Son, S.W., Correa, G.J., Polvani, L.M., 2014. The response of extratropical cyclones in the Southern Hemisphere to stratospheric ozone depletion in the 20th century. Atmosph. Sci. Lett. 15 (1), 29–36. doi:10.1002/asl2.482.

Hauchecorne, A., Godin, S., Marchand, M., Heese, B., Souprayen, C., 2002. Quantification of the transport of chemical constituents from the polar vortex to midlatitudes in the lower stratosphere using the high-resolution advection model MIMOSA and effective diffusivity. J. Geophys. Res. 107 (D21), 3. doi:10.1029/2001JD000491.

Inpe, 2019. Environmental Information System Integrated With Environmental Health. National Institute for Space Research. http://www.inpe.br.

Kim, J.H., Newchurch, M.J., 1998. Biomass-burning influence on tropospheric ozone over New Guinea and South America. J. Geophys. Res. 103 (D13), 1455–1461. doi:10.1029/97JD03048.

Kim, J., Cho, H.K., Mok, J., Yoo, H.D., Cho, N., 2013. Effects of ozone and aerosol on surface UV radiation variability. J. Photochem. Photobiol. B 119 (1), 46–51. doi:10.1016/j.jphotobiol.2013.06.005.

Levelt, P.F., Hilsenrath, E., Leppelmeier, G.W., Van den Oord, G.H.J., Bhartia, P.K., Tamminen, J., Haan, J.F., Veefkind, J.P., 2006a. Scientific objectives of the Ozone Monitoring Instrument. IEEE Transac. Geosci. Remote Sens. 44 (5), 1199–1208. doi:10.1109/TGRS.2006.872336.

Levelt, P.F., Van den Oord, G.H.J., Dobber, M.R., Malkki, A., Visser, H., Vries, J., Stammes, P., Lundell, J.O.V., 2006b. The ozone monitoring instrument. IEEE Transac. Geosci. Remote Sens. 44 (7), 1093–1101. doi:10.1109/TGRS.2006.872336.

R Core Team, 2021. A Language and Environment For Statistical Computing. R Foundation for Statistical Computing. https://www.R-project.org/.

Solomon, S., Ivy, D.J., Kinnison, D., Mills, M.J., Neely, R.R., Schmidt, A., 2016. Emergence of healing in the Antarctic ozone layer. Science (1979) 353 (6296), 269–274. doi:10.1126/science.aae0061.

Sousa, A.J., Silva, R.R., Oliveira, R.D., 2020a. Seasonal and interannual variability of total column ozone in Campo Grande. MS, Brazil. Atmospheric Res. 236, 104833. doi:10.1016/j.atmosres.2020.104833.

Sousa, C.T., Leme, N.M.P., Martins, M.P.P., Silva, F.R., Penha, T.L.B., Rodrigues, N.L., Silva, E.L., Hoelzemann, J.J., 2020b. Ozone trends in equatorial and tropical regions of South America using Dobson spectrophotometer, TOMS, and OMI satellite instruments. J. Atmos. Sol. Terr. Phys. 203, 105272. doi:10.1016/j.jastp.2020.105272.

Souza, A., Aristone, F., Fernandes, W.A., Oliveira, A.P.G., Olaofe, Z., Abreu, M.C., Oliveira, J.F., Cavazzana, G., Santos, C.M., Pobocikova, I., 2020b. In: Analysis of Ozone Concentrations Using Probability Distributions, 42. Science & Engineering, Ozone, pp. 539–550. doi:10.1080/01919512.2020.1736987.

Souza, A., Oliveira-Júnior, J.F., Abreu, M.C., Cavazzana, G.H., 2022a. Spatiotemporal variability of the ozone column over the Brazilian Midwest from satellite data from 2005 to 2020. Water, Air, Soil Pollut. 233, 59. doi:10.1007/s11270-022-05532-w.

Souza, E.O., Oliveira, M.S., Oliveira, J.F., Góis, G., Oliveira, G.L., Costa, C.E.S., Correia Filho, W.L.F., Santiago, D.B., 2021. Estimation and spatialization of erosivity in climatic mesoregions in the State of Alagoas. Revista Brasileira de Meteorologia 35, 769–783. doi:10.1590/0102-77863550005.

Steinbrecht, W., Hegglin, M.I., Harris, N., Weber, M., 2018. Is global ozone recovering? Comptes Rendus Geosci. 350 (7), 368–375. doi:10.1016/j.crte.2018.04.001.

Thompson, A.M., Balashov, N.V., Witte, J.C., Coetzee, J.G.R., Thouret, V., Posny, F., 2014. Tropospheric ozone increases over the southern Africa region: bellwether for rapid growth in Southern Hemisphere pollution? Atmos. Chem. Phys. 14, 9855–9869. doi:10.5194/acp-14-9855-2014.

Toihir, A.M., Portafaix, T., Sivakumar, V., Bencherif, H., Pazmiño, A., Bègue, N., 2018. Variability and trend in ozone over the southern tropics and subtropics. Ann. Geophys. 36 (2), 381–404. doi:10.5194/angeo-36-381-2018.

Wang, J., Ju, T., Li, B., et al., 2024a. Characterization of tropospheric ozone pollution, random forest trend prediction, and analysis of influencing factors in southwestern Europe. Environ. Sci. Eur. 36, 61. doi:10.1186/s12302-024-00863-3.

Wang, T., et al., 2024b. Variability of total ozone column in southwestern Europe: the role of natural and anthropogenic factors. Atmos. Environ. 320, 120987. doi:10.1016/j.atmosenv.2024.120987.

Wang, X., Sun, Y., Tian, D., 2023. Air quality and human health impact assessment of ozone and PM2.5: a case study in a typical urban area in China. J. Clean. Prod. 380, 134952. doi:10.1016/j.jclepro.2022.134952.

Weber, M., Coldewey-Egbers, M., Fioletov, V.E., Frith, S., Wild, J., Burrows, J.P., Long, C.S., Loyola, D., 2018. Total ozone trends from 1979 to 2016 derived from five merged observational datasets: the emergence into ozone recovery. Atmos. Chem. Phys. 18 (3), 2097–2117. doi:10.5194/acp-18-2097-2018.

Wilks, D.S., 2006. Statistical Methods in the Atmospheric Sciences. Academic Press 2nd ed..

Xie, F., Li, J., Tian, W., Zhang, J., Shu, J., 2014a. The impacts of two types of El Niño on global ozone variations in the last three decades. Adv. Atmos. Sci. 31 (5), 1113–1126. doi:10.1007/s00376-013-3166-0.

Xie, F., Li, J., Tian, W., Zhang, J., Shu, J., 2014b. The relative impacts of El Niño Modoki, canonical El Niño, and QBO on tropical ozone changes since the 1980s. Environ. Res. Lett. 9, 064020. doi:10.1088/1748-9326/9/6/064020.

Zhang, J., Tian, W., Wang, Z., Xie, F., Wang, F., 2015. The influence of ENSO on northern midlatitude ozone during the winter to spring transition. J. Clim. 28 (12), 4774–4793. doi:10.1175/JCLI-D-14-00706.1.

Zhang, S., Hu, D., Zhang, J., 2019. The relationship between surface ozone and meteorological parameters in China: a review. Environ. Pollut. 254, 112970. doi:10.1016/j.envpol.2019.112970.